Experimental study on the process of neck cutoff and channel adjustment in a highly sinuous meander under constant discharges

Zhiwei Li [a,b], Xinyu Wu [a], Peng Gao [c,*]

[a] School of Hydraulic Engineering, Changsha University of Science & Technology, Changsha 410114, China
[b] Key Laboratory of Water-Sediment Sciences and Water Disaster Prevention of Hunan Province, Changsha 410114, China
[c] Department of Geography, Syracuse University, Syracuse, NY 13244, USA

ABSTRACT

Neck cutoff is an essential process limiting evolution of meandering rivers, in particular, the highly sinuous ones. Yet this process is extremely difficult to replicate in laboratory flumes. Here we reproduced this process in a laboratory flume by reducing at the 1/2500 scale the current planform of the Qigongling Bend (centerline length 13 km, channel width 1.2 km, and neck width 0.55 km) in the middle Yangtze River with geometric similarity. In five runs with different constant input discharges, hydraulic parameters (water depth, surface velocity, and slope), bank line changes, and riverbed topography were measured by flow meter and point gauges; and bank line migration and a neck cutoff process were captured by six overhead cameras mounted atop the flume. By analyzing the neck cutoff process, development of the cutoff channel, and adjustment of the old channel to cutoff, we found that (i) bank erosion around the upstream and downstream channel segments of the neck reduced its distance, subsequently increased water head gradient on both sides of the neck inducing the occurrence of neck cutoff in a short time period; (ii) the width of the new cutoff channel increased quickly after neck cutoff because the increased local slope generated a higher unit stream power in the cutoff channel; and (iii) neck cutoff significantly increased bank erosion and channel widening in upstream and downstream channels as it is a gradual process compared with chute cutoff. These results suggest that bank revetment around the Qigongling Bend might be necessary to prevent the abrupt occurrence of natural neck cutoff in the future.

© 2018 Published by Elsevier B.V.

1. Introduction

Meander cutoff is a consequence of interaction between internal sinuosity thresholds and external driving factors (e.g., flooding and bank collapse). Cutoff is an integral part of the channel self-regulating process and is a common phenomenon in meandering rivers under various alluvial environments, such as the Mississippi River, upper Yellow River, Tarim River, and Amazonian tributaries (Hooke, 1995; Smith and Winkley, 1996; Gay et al., 1998; Stolum, 1998; Konsoer and Richards, 2016; Wang et al., 2016; Li et al., 2017; Billi et al., 2018). The collapse of a concave bank and point bar deposition along the convex bank push and pull the entire bend to migrate laterally until a cutoff threshold is reached (Seminara, 2006; Parker et al., 2011; Hooke, 2013). Specifically, cutoffs can shorten the length of a river in a short period and limit the sinuosity of a meander planform (Stolum, 1996; Hooke, 2004, 2007; Camporeale et al., 2008). The occurrence of neck cutoff means that the sinuosity of a meander reaches a critical state with the bend narrowed to form a neck. Thus, the difference of water level between the upstream and downstream segments leads to intensive fluvial

erosion in the floodplain when high water level (overbank) flow surpasses the elevation of the neck caused by the appearance of a low-frequency flood (Allen, 1965). If the neck width is much narrower than the average channel width, neck cutoff may be directly triggered by bank collapse. Although numerous flume experiments and field observations have been performed to study the formation and process of chute cutoff (Gay et al., 1998; Micheli and Larsen, 2011; Zinger et al., 2011; Grenfell et al., 2014; Eekhout and Hoitink, 2015; Słowik, 2016; Viero et al., 2018), little has been done to understand the process and mechanism of neck cutoff, in particular, in laboratory flumes.

Laboratory flume experiment is a feasible and controllable method for studying fluvial processes and cutoff of meandering rivers (Friedkin, 1945; Yin, 1965; Schumm and Khan, 1972; Smith, 1998; Braudrick et al., 2009; van Dijk et al., 2012). Many researchers have successfully developed small meandering rivers in laboratory flumes and have observed the phenomenon of chute cutoffs. The earliest laboratory experiment of modeling meandering rivers began in the 1930s (Tiffany and Nelson, 1939). Later, researchers changed the composition of bed materials and added fine-grained material to or planted vegetation in the channel to reproduce meandering channels with high sinuosity. Loess, silt, and fine sand were common materials added to the flume experiment to model the development and evolution of the Mississippi

River in laboratory flumes (Friedkin, 1945). Magnitude and variation of incoming discharges are regarded as primary controlling parameters for the development of a meandering river. For example, Visconti et al. (2010) showed that discharge variability was critical for developing meandering channels. Cohesive materials (e.g., clay, quartz powder, kaolin, diatomaceous earth, and porcelain clay) also play a key role in the formation of a meandering channel because they may deposit on the convex bank, preventing chute cutoff and reducing possibility of bank collapse (Friedkin, 1945; Yin, 1965; Schumm and Khan, 1972; Schumm, 1985; Dulal and Shimizu, 2010; van Dijk et al., 2012; Constantine et al., 2014). Thus, some experiments have successfully produced small meandering rivers by introducing silt or clay material into water flow during flume experiments and studied the effects of flow, sediment, and channel longitudinal gradient on development of meandering rivers (Smith, 1998; Peakall et al., 2007; van Dijk et al., 2012; Han and Endreny, 2014). Natural meandering rivers mostly are covered by composite bank materials with plant roots generally grown in the upper bank layer, which can increase river bank stability, attenuate near-bank velocity, and prevent bank failure, particularly the roots system enhancing the tensile and shear strength of river bank and floodplain (Abernethy and Rutherfurd, 2000; Simon and Collison, 2002; Perucca et al., 2007; Zhu et al., 2018; Krzeminska et al., 2019). Planted alfalfa sprouts in a laboratory flume was a feasible and auxiliary method to fix point bars and river banks, such that formation of continuous bends and the process of chute cutoff may be simulated (Braudrick et al., 2009; Tal and Paola, 2010). In these experiments, the strength provided by alfalfa sprouts was regarded as the necessity for sustaining the meandering of an experimental channel.

Even though many experiments had produced bends in laboratory flume, factors affecting the formation and evolution of a meandering channel are still not fully understood owing to different adaptabilities of meandering rivers in different alluvial environments. In particular, reproducing highly sinuous meandering channels in laboratory flumes is still difficult (Braudrick et al., 2009; Howard, 2009; Güneralp et al., 2012; van Dijk et al., 2012) because their creation in flumes requires a subtle combination of flow conditions (discharge amplitude, variability, and duration), sediment feeding (ratio of coarse sand and fine sand), riverbed slope, and vegetation plantation (alfalfa sprouts). For flow conditions, no consensus has been reached on whether discharge should be constant or variable during the experiment (Braudrick et al., 2009; Visconti et al., 2010). For sediment feeding, though the key role of fine-grained materials has been recognized by many researchers, the appropriate percentage content of fine-grained materials is still in debate (Smith, 1998; Han and Endreny, 2014; van Dijk et al., 2014). Moreover, the appropriate riverbed slope and how it should be matched by bed materials of different grain sizes for generating meandering channel is inconclusive. For vegetation, whether it plays a controlling role in the development of a meandering channel has been controversial. Some believed that the controlling factors in meandering river development are only flow and sediment conditions (Church, 2002; Peakall et al., 2007), whereas others argued that vegetation is a controlling variable (Millar, 2000; Micheli et al., 2004; Perucca et al., 2007; Braudrick et al., 2009; Tal and Paola, 2010).

It is well known that sinuosity of a meandering channel in laboratory flumes is relatively low and only chute cutoff may occur. The sufficient conditions for triggering neck cutoff in a flume are little known in comparison with the flow-sediment and boundary conditions for neck cutoff in natural rivers. One obstacle lies in the fact that point bar typically does not have strong resistance to prevent the occurrence of chute cutoff in a flume (Braudrick et al., 2009; van Dijk et al., 2012). Another is that a high-sinuosity channel with a narrow neck requires a very long time to form from a freely developed, low-sinuosity channel. Flume experiments for investigating neck cutoffs need to reproduce three triggering factors learned from natural meandering rivers (Hooke, 1995, 2004, 2013; Thompson, 2003; Howard, 2009; Li et al., 2017): (i) point bar deposition around the inner bank should have a

similar rate to that of the outer bank erosion, which is typically achieved by a composite bank with higher resistance in the upper than in the lower layers, such that the upper collapsed blocks can temperately protect the bank and reduce bank erosion rate; (ii) magnitude and duration of discharges should be variable; (iii) sediment transport rate should be variable, specifically, high in flood season, low and nearly zero during the dry season. Clearly, if these conditions are not met, creating a high-sinuosity channel and triggering neck cutoff in laboratory flumes would be difficult. Alternatively, it might be much easier to create a high-sinuosity channel as a prerequisite based on a real or sine-generated meandering river (Song et al., 2016; Xu and Bai, 2013), and then reproduce neck cutoff under appropriate hydraulic conditions in the flume. For instance, a neck cutoff was successfully triggered in a small-scale flume (3.7 m long and 1.8 m width) (Han and Endreny, 2014). Nonetheless, this study mainly focused on head gradients and hyporheic exchange during neck cutoff without investigating the critical flow conditions of neck cutoff.

In our flume experiments, we successfully created the process of neck cutoff that may occur in the Qigongling Bend of the Jingjiang River in a channel of a similar planform at the 1/2500 reduction geometrical scale. The studied channel is the middle reach of the Yangtze River, from Zhicheng station in Hubei Province to Chenglingji station in Hunan Province, referred to as the Jingjiang reach with a length of about 350 km (Fig. 1A). The Qigongling Bend (13 km long and 1.2 km wide) at the end of the Jingjiang reach is located at the outlet of the Dongting Lake, which is the second largest freshwater lake in China. The downstream neck is only 10 km away from the junction of the Yangtze River and Dongting Lake. Thus far, the narrowest neck width of the Qigongling Bend is 550 m on average (Fig. 1B). Since the initial impoundment of the Three Gorges Reservoir in 2003, the sediment-starved flow coming to the Jingjiang River reach has accelerated the rate of bank collapse, largely increasing the possibility of neck cutoff in the Qigongling Bend in the future, assuming no bank protection is implemented. This possible neck cutoff could cause an extremely negative effect on channel stability of the lower Jingjiang River and hydrological regime of the Dongting Lake.

The objective of this experimental study is to capture the detailed process of neck cutoff that may occur in such a highly sinuous meander bend, to estimate the critical hydraulic condition of neck cutoff, and to examine the associated channel adjustment. First, we provide a detailed description of the experimental flume and layout, boundary conditions of experiments in the laboratory, measuring instruments, and data processing method. Second, we present hydraulic characteristics of five experimental runs. Third, we depict the process of neck cutoff and the development of the cutoff channel. Fourth, we examine the adjustment of the upstream, bend, and downstream channel segments. Finally, we point out limitations and the implication of our neck cutoff experiments and discuss the conditions and processes of neck cutoff in comparison with chute cutoff experiments.

2. Study reach and method

2.1. Study reach

The lower Jingjiang River is located at the tail of the ancient Yunmeng Delta, in which the river developed on the Holocene alluvial and lacustrine sedimentary layers (Zhou, 1994). The lower Jingjiang River is an alluvial meandering channel (Fig. 1), about 175 km long with a sinuosity of 1.87 and channel slope of 0.0175‰. It has undergone a complicated evolution process and artificial cutoff engineering since the 1860s (Pan et al., 1978), which left nine bends fully or partially constrained by the Jingjiang levee. Bed materials are mostly sand, underlain by a pebble-gravel layer. River bank consists of a composite of two-layer materials, relatively fine sand in the lower layer and silty clay (several meters) in the upper layer. Although most bends at the end of Jingjiang River are confined within the Jingjiang levee,
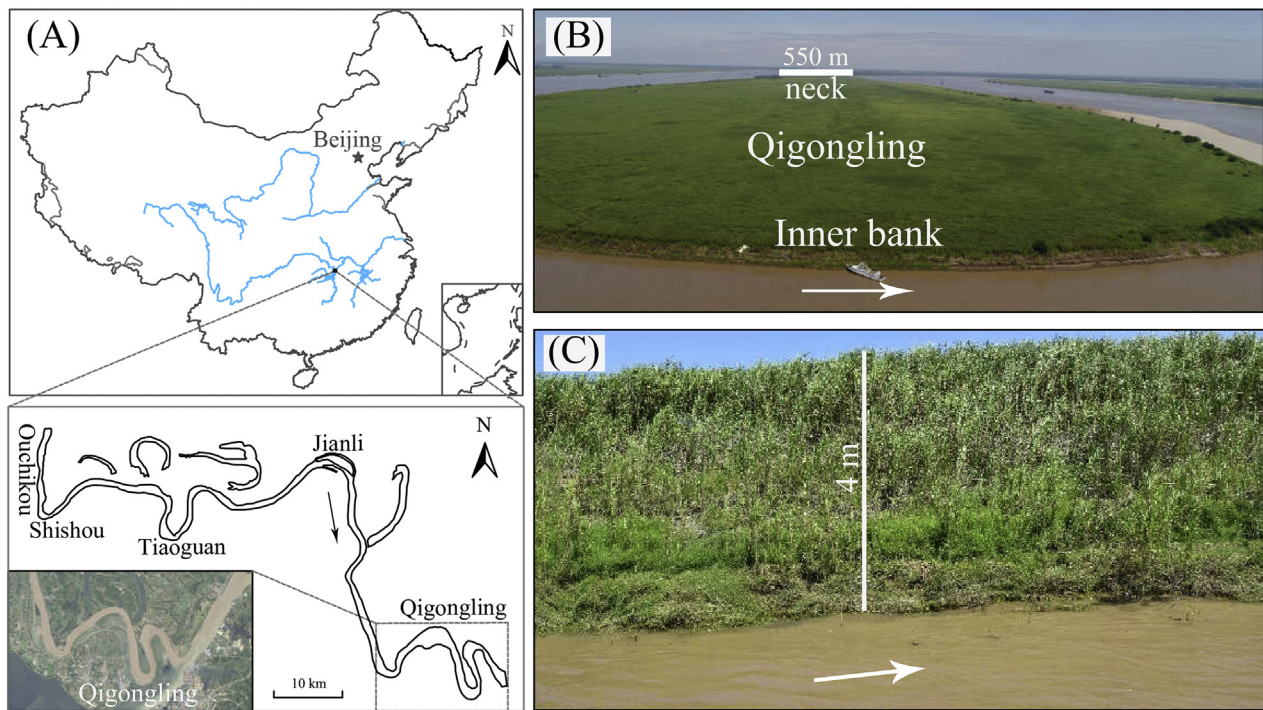
Fig. 1. General settings of the study area. (A) Location of the lower Jingjiang River and Qigongling Bend in the middle Yangtze River; (B) bird's eye view photo of the bend taken by an unmanned aerial vehicle on 29 August 2017; (C) representative vertical profile of the inner bank of the Qigongling Bend.

the Qigongling Bend has not been limited by a revetment project (Fig. 1B and C).

Since the impoundment of the Three Gorges Reservoir in 2003, incoming flow and sediment load supplied to the lower Jingjiang River shows a significant local adjustment, highlighted by riverbed scouring and bank collapse (Jia et al., 2010; Xia et al., 2014, 2017). The neck width is further shortened by bank collapse with a retreating rate of about 12.5 m/year, which was estimated by multiyear remote sensing images (Google Earth and Landsat) (Yang et al., 2015). Thus, there is a high possibility in the following 10–20 years that a neck cutoff in this bend may occur given that no bank revetment projects are available. The potential cutoff will generate strong riverbed erosion because of significantly increased local channel slope and hence greatly alter the hydrological regime at the entrance of Dongting Lake. The study reach contains seven bends in the upper and lower reaches of the Qigongling Bend, and its total length is 53 km (Fig. 1). The floodplain and bank within the Qigongling Bend are covered by dense reed about 3 m high (Fig. 1B and C).

2.2. Flume setup and experiment procedures

2.2.1. Flume setup

Experiments were conducted in a flume built between 2016 and 2017 in the Center of Hydraulic Engineering at Changsha University of Science & Technology, China. It is 25 m long, 6 m wide, and 0.4 m deep and has an experimental section 21.5 m long with a mobile bed (Fig. 2A and B). A head tank has a trapezoidal shape with the short edge, long edge, width, and depth of 2.2, 6.0, 2.2, and 0.6 m respectively. It is connected via a grille made of bricks to a rectangular pool of 1.8 m long, 6 m wide, and 0.4 m deep at the flume inlet to assure that flow entering the flume is steady (Fig. 2A). Input flow is supplied by a centrifugal pump and adjusted using a valve to reach the designed input discharge, which subsequently remained unchanged to keep the constant discharge in each run. The discharge is measured by an electromagnetic flow meter with the accuracy of 0.001 m³/h. Clear water with constant discharge was used in experiments to mimic the current

sediment-starved flow in the Qigongling Bend. During experiments, water flowed through the pump into the head pool and subsequently entered the channel through the inlet equipped with an energy dissipation grid at the bottom to alleviate erosion around the inlet (Fig. 2C). The flume outlet is connected to a sediment settling pool of 2 m long for collecting sediment and a tail water pool of 1.5 m long (Fig. 2A). A tailgate that is 0.3 m wide and 0.1 m deep is installed in the center of the flume tail, directing water and sediment in the flume to the settling tank (Fig. 2D). The mobile bed in the flume consists of a sediment layer with a thickness of 0.2 m (Fig. 2B). The sediment is quartz sand with a median size $d_{50} = 0.327$ mm and a non-uniform coefficient $\varphi = \sqrt{d_{75}/d_{25}} = 1.413$. Sediment size distribution (Fig. 3) was determined using a laser particle size analyzer (Mastersizer 2000).

Six video cameras (4 million pixels, HIKVISION DS-2CD3T45D-I3) were installed atop the centerline of the flume at the height of 7 m, to record real-time morphological changes of the channel in the experimental section. The distance between two adjacent cameras is 2.89 m, and each camera covers a zone of 3.56 m long, such that the entire 21.5-m experimental section may be covered by all cameras. A metal flatter that can be lifted in front of an automatic vehicle over the bed can smoothly scrape the movable bed to obtain a flat mobile bed with a designed slope (Fig. 2B). It achieves this function by moving on steel rails installed on two sidewalls of the flume. Along the back side of an automatic vehicle, a row of point gauges (which can be moved transversely) was installed to measure water level and cross section topography. Two rows of 110 planimetric control points were set at the interval of 0.5 m in the longitudinal direction of the flume to control the accuracy of initial channel planform. Control points were added at places where channel planform changes greatly.

Prior to each experimental run, the mobile bed was leveled to a designed gradient by the flatter. Then, the geometric planform of the Qigongling Bend was reduced at the 1/2500 scale to that of the initial channel in the flume (see Fig. 2B). Cross sections of the initial channel were approximately rectangular, 10 cm deep, 0.2–0.8 m wide; and the initial width-depth ratios ranged from 0.2 to 0.8. Notably, this study only considered the geometric similarity to the Qigongling Bend. The
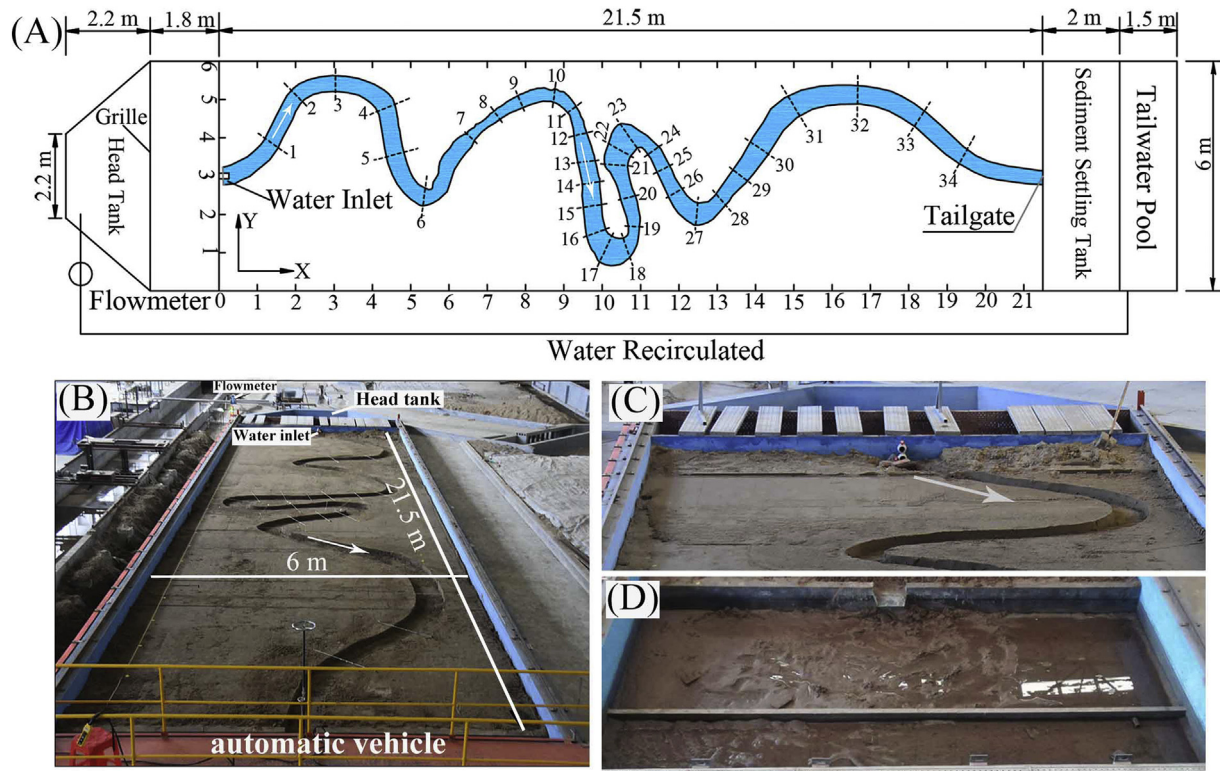
Fig. 2. Experimental flume and layout: (A) setup of the experimental flume and the studied high sinuous meandering channel, (B) upstream view of the initial channel, (C) close view of the flume inlet, (D) close view of the flume outlet and sediment settling pool. The experimental section was divided by the upper segment (S7–S13), middle segment (S13–S21), and lower segment (S21–S26), a representative cross section within each was identified as S11, S18, and S24 respectively.

hydraulic similarity could not be achieved in this case for two reasons. First, hydraulic information, such as mean flow velocity and depth, and bedform sizes and their spatial distribution, is not available. Second, even referring to the data from the nearest downstream gauging station, hydraulic similarity requires that the water depth in our flume should be only 1 cm, which is not even high enough to generate fluvial erosion of the quartz sand (2650 kg/m^3, D_{50} = 0.327 mm) used in our flume experiments. The created channel involved seven bends, numbered in order from upstream to downstream. A total of 34 cross sections spaced by distances ranging between 0.42 and 2.00 m along the channel were selected for measurements during each run (Fig. 2A). To avoid the boundary effect from upstream and downstream sections, the studied

area was selected as the middle reach, which began at cross section 7, denoted as S7, and ended at cross section 26, denoted as S26 (Fig. 2A).

2.2.2. Experiment design and measurement

Before starting the formal experiments, we conducted a series of experiments with discharges increasing from low to high. These preliminary experiments allowed us to learn the possible ranges of discharges that may or may not cause a neck cutoff. Based on this knowledge, we designed five runs that had constant discharges of 0.5, 1.5, 2.0, 2.5, and 3.0 L/s with three channel slopes (i.e., RUN1, RUN2, RUN3, RUN4, and RUN5 in Table 1). These runs had different mean water depth and velocity and different experimental durations. The mean shape of the initial channel in different runs was similar with the same width/depth ratio of 4.38, though local variations existed in each run. When neck cutoff occurred, its location was always near the narrowest neck of bend 4 that was 0.22 m long (Fig. 2A). Duration of neck cutoff in each run is defined as the lasting time from the beginning of the experiment to the moment when intersection of the neck upstream-downstream channel occurred. At the beginning of this duration, the ratio of the narrowest neck width to the average channel width is roughly 0.4 in all runs.

The initial topography of S7–S26 was measured before the experiment. After neck cutoff occurred, the input discharge was halted and their topography was measured again, after which the experiment was resumed until the channel width did not change and banks no longer receded on average. The topography of these cross sections was measured again after the experiment stopped. Water level, depth, and cross section topography were measured using point gauges at an accuracy of 0.1 mm. Surface velocity was measured using a hand held surface velocity radar (Decatur Electronics, UK) with the accuracy of ±0.03 m/s. During experiments, these variables at each cross section were measured every 12 h before the occurrence of neck cutoff and in variable intervals in different runs after cutoff depending on the
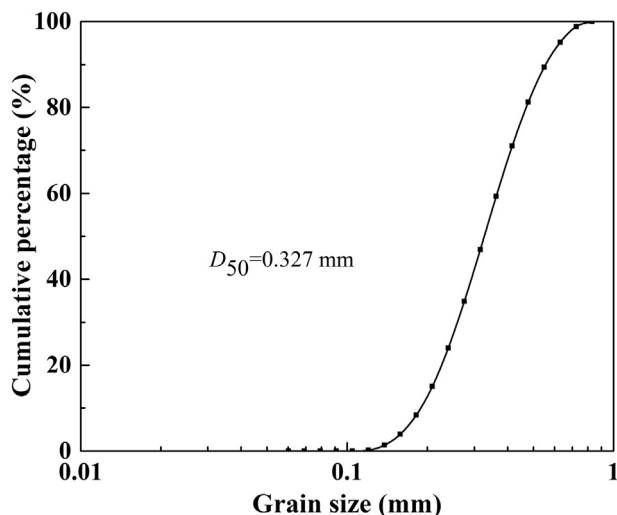

Fig. 3. Grain size distribution of sediment materials used in flume experiments.

Table 1
Initial and boundary conditions of four designed runs.

Run	Discharge Q (L/s)	Initial slope S_r (‰)	Mean channel width in the end of the run (m)	Mean water depth in the end of the run (m)	Mean velocity (m/s)	Initial channel width/depth (W/H)	Duration (h)
RUN1	0.5	1.0	0.468	0.029	0.04	4.42	13.00
RUN2	1.5	1.0	0.471	0.038	0.09	4.44	78.00
RUN3	2.0	1.0	0.476	0.041	0.11	4.51	85.45
RUN4	2.5	0.8	0.475	0.046	0.12	4.47	108.25
RUN5	3.0	1.7	0.471	0.054	0.12	4.65	41.00

duration of the experiment. For runs 3–5 in which neck cutoff occurred, local channel slope around the cutoff position was also measured immediately after neck cutoff and used to calculate stream power per unit length P (N·s^{-1}):

$$P = \gamma Q S \tag{1}$$

where, γ is water gravity density, 9800 N/m^3; Q is input discharge, m^3/s; and S is local channel slope.

At the end of each run with cutoff, topography of a representative cross section in the new channel was measured as well. The width/depth ratio of each cross section was calculated using the measured topography. The studied channel was divided into three segments, the upstream (S7–S13), the bend (S13–S21), and the downstream (S21–S26) segments (Fig. 2A). Segments S11, S18, and S24 were selected as representative cross sections for the three segments, and their width/depth ratios were then calculated to reflect morphological characteristics of these segments.

Morphological changes and bank lines in the experimental flume were captured in real-time by six video recorders with the maximum geometrical distortion error of 0.12 m. The distortion of images was corrected using Adobe Photoshop software. Based on recorded images, the following variables were determined:

- Neck width. In general, it was measured every 1 or 2 h in each run.
- Cutoff channel width (measured in runs 3–5). At the first hour after cutoff, it was measured in minutes because of its fast widening rate and then in the duration of 1 h. The channel widening rate was subsequently calculated using these values.
- Channel centerline. The position of the channel centerline was delineated at the moments when it was significantly different from its earlier positions during each experiment. The channel migration rate was subsequently calculated using these centerlines. Each centerline was also classified into the three segments defined previously. The migration rate for each segment was calculated as the mean distance of centerlines along all selected cross sections within each segment between two moments.
- Scour area. It was calculated using the delineated centerlines for each of the three segments as the difference between the area of one moment and that of the previous moment.

Each of these five experimental runs was not repeated for three reasons. First, the initial conditions of a meandering channel in a flume of this size for each run is essentially not repeatable. Before each run, the meandering channel with designed width, depth, and bed slope was created manually on the presmoothed loose sand bed. Given that the channel extended for >21 m, assuring exactly the same width, depth, and bed slope is almost impossible. As a result, even if the same water discharge is supplied in a repeated run, the hydraulic variables and bedforms will not be the same as those in the previous run. Consequently, the possible different experimental results (e.g., the time of cutoff occurrence and local stream power at the cutoff moment) between this and previous runs may be caused by the different initial conditions of the two runs, rather than possible randomness in each run. Second, the purpose of our experiments was to reveal the process of neck cutoff occurrence, rather than predicting when a neck cutoff will

occur. Thus, a repeated RUN1 will not change the nature that this run does not trigger a neck cutoff, though specific hydraulic results, such as mean flow velocities and depths at different time steps during the experiment, may be different between the two runs. Third, previous flume experiments aiming at revealing mechanisms of chute cutoff and lateral migration used the same strategy as that adopted in our experiments: do not repeat the same experimental run (Smith, 1998; Braudrick et al., 2009; Dulal and Shimizu, 2010; van Dijk et al., 2012; Xu and Bai, 2013; Song et al., 2016). Apparently ignoring the repeatability issue of flume experiments for exploring mechanics of fluvial processes has become a common practice.

3. Results and analysis

3.1. Hydraulic characteristics and adjustment before and after cutoff

The longitudinal changes of water depths in the five runs generally showed oscillating patterns with the magnitude of the change increasing orderly from 1 cm in RUN1 to 3 cm in RUN5 (Fig. 4A), indicating that these changes were mainly controlled by the magnitudes of input discharges. In the upstream segment between 0 and 5.1 m (i.e., from S7 to S13), changes of water depths in runs 3–5 with neck cutoff were significantly higher than those in runs 1 and 2 without neck cutoff. Also, water depth increased with time in the former runs and decreased in the latter ones. Because this segment was upstream of the location where neck cutoff occurred, the different trends of water depth changed between runs with and without neck cutoff were apparently irrelevant to the process of neck cutoff. In the downstream segment between 9.89 and 16.20 m (i.e., from S21 to S26), no discernable discrepancy may be identified between the oscillating patterns of runs 3–5 and those of runs 1 and 2. In the segment between 5.10 and 9.89 m (i.e., from S13 to S21), the oscillating pattern persisted in runs 1 and 2 with no cutoff events, but water depth tended to increase over time in most parts of the segment. For runs 3–5, this segment represented the abandoned channel after neck cutoff. The change of water depth after and before neck cutoff within this segment still had the oscillating pattern, and most parts of the segment experienced water depth increase. This similar pattern indicated that though a proportion of incoming flow was diverted to the cutoff channel, the pattern of longitudinal water depth change in the abandoned channel was still not affected. Over the entire study channel reach (i.e., from S7 to S26), the range of the absolute values of water depth changes, which varied between 0 and 2.73 cm was comparable to that of the heights of ripples and dunes developed in these experiments, which was from 1.0 to 3.5 cm. Thus, the oscillating patterns of water depth changes along the reach was more likely caused by downstream movement of ripples and dunes and were not related to the processes of neck cutoff.

Specifically, in runs 1 and 2, time averaged water depths in three cross sections (i.e., S10, S18, and S23) located at the apex of bends 3, 4, and 5 (Table 2) showed that as the channel evolved, water depth generally decreased except for S23 in RUN1. In runs 3–5, water depth after neck cutoff were generally higher than those before for all three cross sections (Table 2). Although neck cutoff reduced water discharges in the abandoned channel (i.e., S18), water depth in S18 still increased after neck cutoff because the concave bank section in S18 experienced
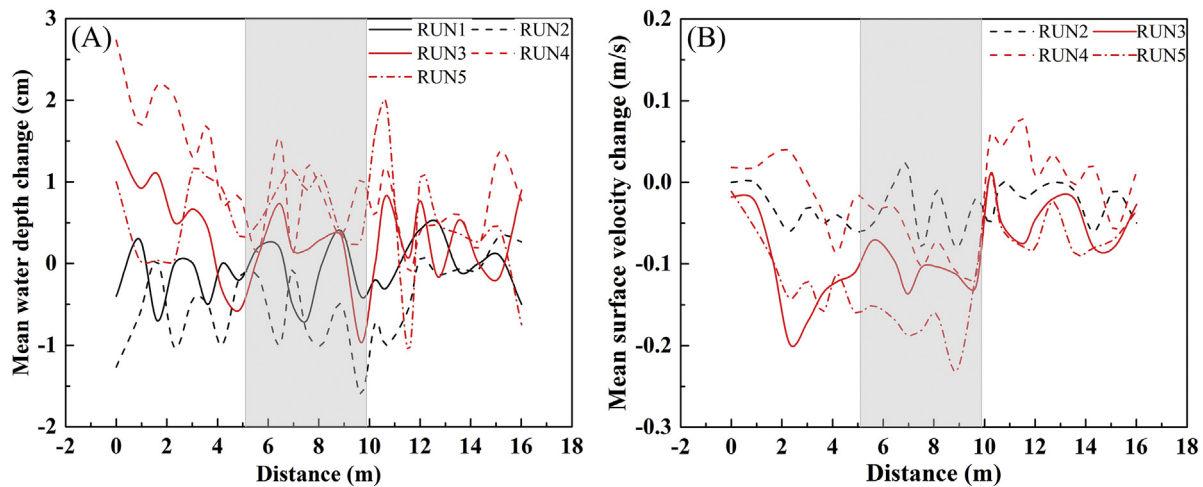
Fig. 4. Longitudinal variations of time-averaged water depth and surface velocity in five runs (the gray zone represents the bend segment between S13 and S21). The considered time periods for runs 1–5 were 6th–12th h, 24th–48th h, 34.95th–59.45th h, 70th–91.25th h, and 5th–28th h respectively.

downward cutting before the cutoff, which led to its higher water depth than that in other sections. Furthermore, standing water in the abandoned channel, because it cannot flow out at the downstream end of the neck cutoff, also contributed to the higher water depth. These results were consistent with those along the study reach.

Surface velocity, however, showed a diverse trend in two ways (Fig. 4B). First, changes of surface velocity varied around the mean (i.e., −0.029 m/s) over the entire study reach in RUN2 without neck cutoff. Second, in runs 3–5 with neck cutoff, changes of surface velocity in the abandoned segment (i.e., from 5.10 to 9.89 m) were generally lower than those in the downstream segment (i.e., from 9.89 to 16.20 m). This difference possibly demonstrated the influence of neck cutoff on surface velocity in the abandoned channel. Specifically, surface velocity in the three cross sections illustrated two types of discrepancies between RUN2 and runs 3–5. In S10 and S23, surface velocity in RUN2

decreased moderately (18% and 2.3% respectively). Yet, in RUN3 to 5, it could either decrease by 51% (RUN3), increase by 38% (RUN4), or both (RUN5). In S18, surface velocity in the three runs with neck cutoff (i.e., runs 3–5) showed great decrease after cutoff by 65%, 75%, and 86%, respectively (Table 2); while in RUN2 without neck cutoff, it was merely reduced by 20%. Overall, surface velocity was apparently more sensitive to neck cutoff than water depth.

3.2. Process of neck cutoff and cutoff channel development

3.2.1. Process of neck cutoff in different flume experiments

Neck cutoff did not happen in runs 1 and 2. Consequently, the neck width never became zero in these two runs (Fig. 5). In RUN1, the lowest input discharge (Table 1) induced little bank erosion around the neck. As such, this width almost remained the same during the entire experimental period (Fig. 6A). In RUN2, the relatively higher input discharge (Table 1) caused limited bank erosion, giving rise to the decrease of the neck width, which kept it about 17% less than the original value (i.e., 0.22 cm) at the end of the experiment (Figs. 5 and 6B).

Neck cutoff occurred in runs 3–5. In RUN3, the neck width reduced quickly at the rate of 0.008 m/h in the first 12 h. Then, in the following 16 h, the reduction rate drastically dropped to 0.00092 m/h, which was followed by an increased reduction rate of 0.0055 m/h until the

Table 2
Average water depth and surface velocity of S10, S18, and S23 over time.

| Run	Section	Average water depth (cm)		Average surface velocity (m/s)	
		$t = 6$ h	$t = 12$ h	$t = 6$ h	$t = 12$ h
RUN1	S10	2.00 ± 0.71	2.03 ± 0.56		
	S18	2.33 ± 0.62	2.27 ± 0.53		
	S23	2.07 ± 0.33	2.20 ± 0.37		
		$t = 24$ h	$t = 48$ h	$t = 24$ h	$t = 48$ h
RUN2	S10	3.83 ± 1.25	2.80 ± 0.50	0.149	0.122
	S18	4.33 ± 0.24	3.50 ± 1.22	0.180	0.144
	S23	4.83 ± 0.24	3.83 ± 0.85	0.171	0.167
		15.5 h before cutoff	9 h after cutoff	15.5 h before cutoff	9 h after cutoff
RUN3	S10	2.53 ± 1.46	3.03 ± 0.81	0.330	0.132
	S18	3.83 ± 1.31	4.33 ± 1.65	0.160	0.056
	S23	4.00 ± 1.47	5.83 ± 1.65	0.290	0.240
		11.25 h before cutoff	10 h after cutoff	11.25 h before cutoff	10 h after cutoff
RUN4	S10	3.17 ± 1.65	4.63 ± 2.19	0.167	0.205
	S18	5.33 ± 2.49	5.85 ± 2.62	0.138	0.035
	S23	3.83 ± 2.39	5.03 ± 1.23	0.115	0.159
		14 h before cutoff	9 h after cutoff	14 h before cutoff	9 h after cutoff
RUN5	S10	2.88 ± 1.58	3.47 ± 1.31	0.298	0.156
	S18	5.97 ± 1.20	6.00 ± 1.47	0.210	0.029
	S23	4.73 ± 0.61	4.27 ± 1.72	0.138	0.182
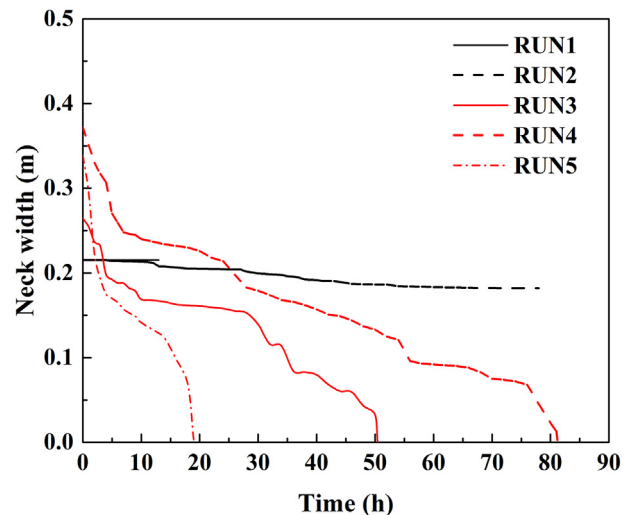
Fig. 5. Changes of the neck width over time in all five runs.

Fig. 6. Illustration of the bend evolution in the five experiments. (A and B) Planform of runs 1 and 2 at the 7th and 48th hour respectively; (C and D) the planforms of runs 3–5 at their occurrence of neck cutoff.

50th hour. The neck width at this time was 0.0325 m. This width was swiftly eroded within the next 27 min, triggering the occurrence of neck cutoff (Figs. 5 and 6C). In RUN4, the neck width reduced even faster at the rate of 0.0158 m/h in the first 8 h. Subsequently, the neck width was reduced with a relatively constant but much lower rate of 0.0026 m/h for a relatively long time to the 76th hour. In the following 5 h, the neck width decreased at a relatively higher rate of 0.011 m/h, reaching 0.013 m. It only took 15 min to erode this short distance and initiate neck cutoff (Figs. 5 and 6D). In RUN5, the neck width reduced with the highest rate of 0.0338 m/h compared with that in runs 3 and 4 for the 5 h from the beginning of the experiment. Then, the width reduction was slowed down with the rate of 0.0067 m/h in the following 7 h and was increased again to the rate of 0.0138 m/h until around the 18th hour when the neck width was 0.068 m. It took about 1 h for flow to erode this distance to start neck cutoff (Figs. 5 and 6E). The duration

to neck cutoff was 50.45, 81.25, and 19 h for runs 3, 4, and 5 respectively. Despite different durations, the process of neck cutoff in the three runs was generally manifested by bank erosion on both sides of the neck whose rates may be characterized by a similar trend: a high rate within the first 30% of the duration, a low rate in the following >40% of the duration, a relatively high rate of the remaining time of duration with a sharply increased rate at the end of the duration, indicating the fact that a neck cutoff may develop for a long time but its occurrence is often in a very short time period, making it very hard to capture in reality.

3.2.2. Evolution of the new channel after neck cutoff

After cutoff, the development of the new channel went through three phases: neck intersection, channel widening, and channel stabilization (Fig. 7). Immediately after neck cutoff, the connected neck was
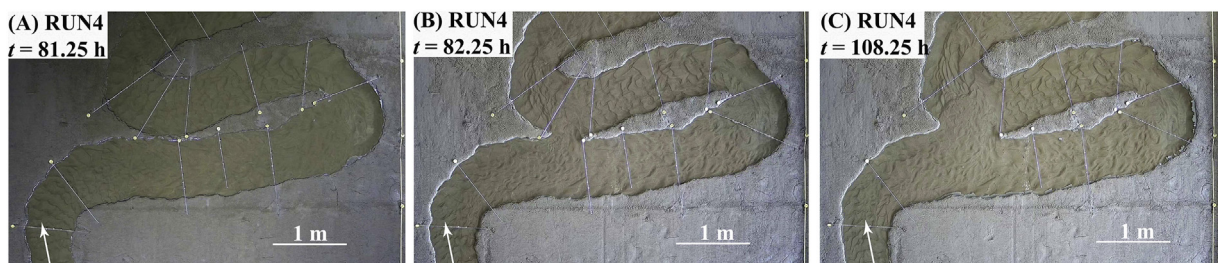

Fig. 7. Evolution of the cutoff channel (using RUN4 as an example): (A) the occurrence of cutoff, (B) the formation of a new cutoff channel, and (C) final stage of the channel.
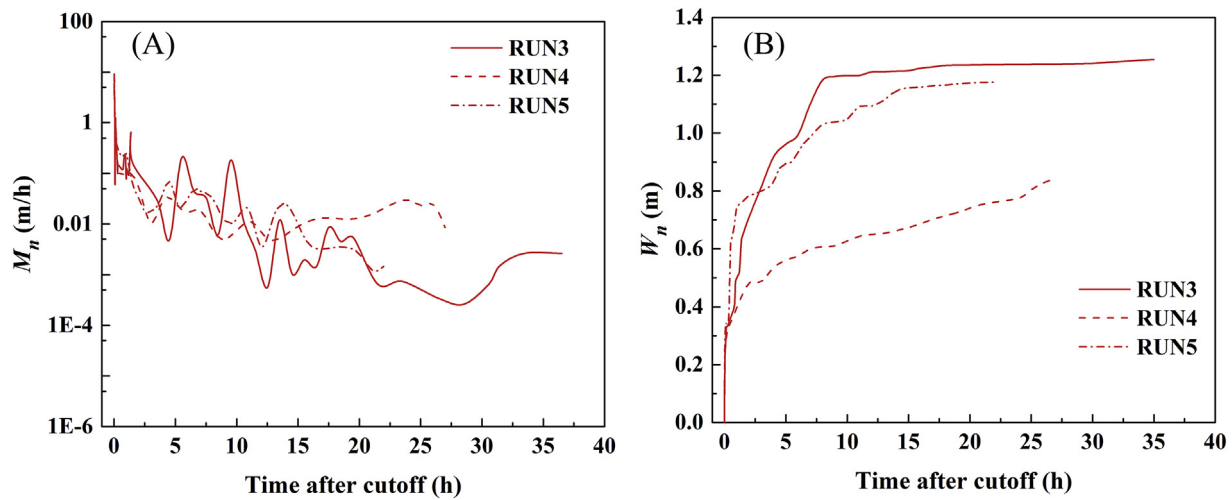
Fig. 8. Development of the cutoff channel in runs 3–5: (A) changes of the widening rate of the cutoff channel after neck cutoff, and (B) the width change of the new channel.

scoured and widened promptly, causing neck intersection to end within a few minutes. In RUN3, just after cutoff, the widening rate M_n of the connected neck was 6.04 m/h (Fig. 8A), which meant that the connected neck was widened by 0.101 m within 1 min. In runs 4 and 5, this rate was 8.15 and 9.11 m/h respectively, which corresponded to the broadening width of 0.136 and 0.152 m in the first minute, respectively. In the following 5 to 10 min, this rate plunged to 0.5 m/h. Nonetheless, the width of the new channel W_n still increased very fast within this time period in all three runs, leading to W_n = 0.329, 0.292, and 0.343 m for runs 3, 4, and 5 respectively, 10 min after neck cutoff marking the end of the first phase (Fig. 8B).

In the channel widening phase, the widening rate further reduced to <0.05 m/h after about 5.5, 2.0, and 1.5 h in runs 3, 4, and 5 respectively (Fig. 8A). With these rates, W_n increased to 0.962, 0.603, and 0.902 m respectively, 5.5 h after neck cutoff. Subsequently M_n continuously reduced to 0.01 (m/h) 10 to 11 h after neck cutoff in runs 3–5, giving rise to W_n = 1.128 m for RUN3 at the 8th hour, W_n = 0.806 m for RUN4 at the 24th hour, and W_n = 1.146 m for RUN5 at the 14th hour (Fig. 8B). Comparing with the first phase, values of M_n were vastly reduced in the second phase (Fig. 8A), and correspondingly those of W_n remained relatively high increase rates (Fig. 8B). After about the 11th hour, M_n gradually approached zero with the approaching rate decreased in the order of runs 3–5 (Fig. 8A). The consequence of these different approaching rates may be reflected by different patterns of width widening. For RUN 3, W_n gradually increased to the final value of 1.254 m at the 37th hour after neck cutoff, for runs 4 and 5, it increased to 0.836 and 1.175 m/s at the end of the experiment, respectively. This long period with slow growth of W_n featured the third phase of channel development.

Different evolution paths of the new cutoff channel in runs 3–5 (Fig. 8B) produced different channel cross section morphology (Fig. 9). The cross section in RUN3 was generally shallow and wide with the thalweg developed at the right bank. That in RUN4 was narrower and deeper with the thalweg located at the left bank. In RUN5, the cross section had a similar width and the location of the thalweg to those in RUN3, but different bed topography. The ratio of width to depth for runs 3, 4, and 5 was 44.91, 20.75, and 37.79 respectively. Apparently, values of this ratio were sufficient to characterize the morphological differences among the three cross sections.

3.3. Impact of neck cutoff on channel morphodynamics

3.3.1. Channel lateral migration

Because neck cutoff did not happen in RUN2, temporal changes of lateral migration of the upstream, bend, and downstream segments

(i.e., S7–S13, S13–S21, and S21–S26) showed identical trends. In 24 h after the beginning of the experiment, the three segments experienced higher migration rates M_c of 1.28, 0.62, and 0.72 mm/h, respectively (Fig. 10A). Values of M_c decreased greatly to 0.66, 0.35, and 0.42 mm/h respectively, 24 h later. The decreasing trend continued to the 72nd hour with a lower degree for the upstream segment, reaching 0.59 mm/h and a higher degree for the other two segments, reaching 0.22 and 0.16 mm/h respectively. Toward the end of the experiment, the upstream segment still decreased to 0.57 mm/h, while the bend and downstream ones increased to 0.30 and 0.18 mm/h respectively. Among the three segments, the upstream one had the highest degree of lateral migration.

In runs 3–5, the occurrence of neck cutoff altered the temporal trends of lateral migration of the three segments differently. Before neck cutoff in these runs, values of M_c in all three segments still showed decreasing trends, similar to that in RUN2, though the decreasing rate varied from runs 3–5 (Fig. 10B–D). The cease of migration of the abandoned segment after neck cutoff existed in runs 3–5 because of obvious reasons: significant reduction of flow due to flow diversion to the new channel and sediment plug at the entrance of the abandoned channel. For the upstream segment, cutoff in RUN3 enhanced its migration rate
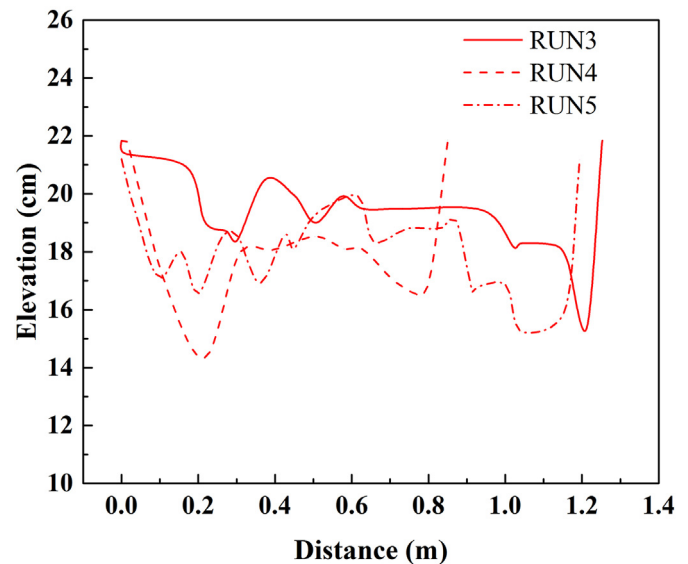

Fig. 9. Final cross section profiles of the cutoff channel in the three runs with neck cutoff (i.e., runs 3–5).
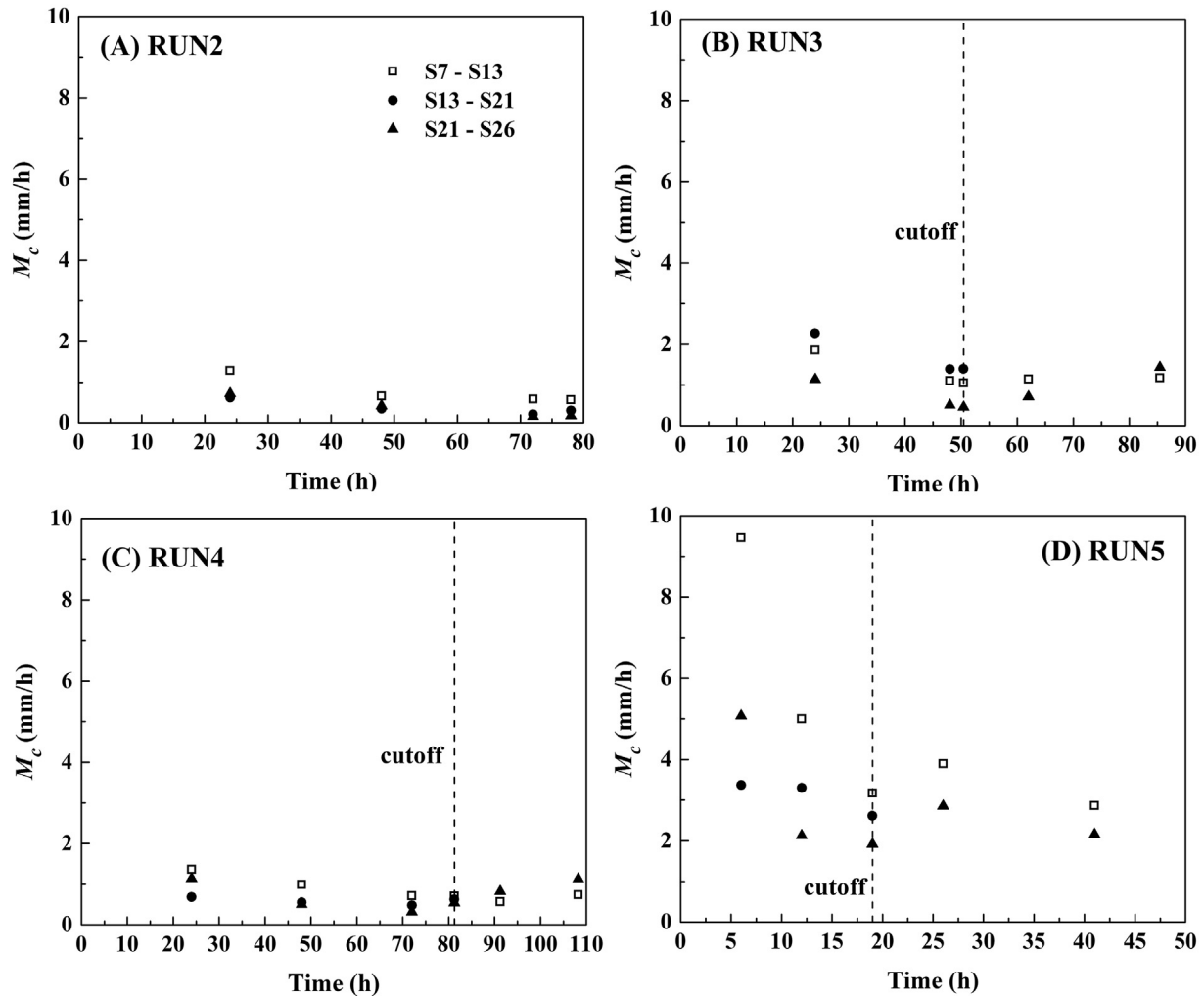
Fig. 10. Changes of migration rates over time in runs 2–5.

evidenced by the increase of M_c values in the remaining experimental time (Fig. 10B). Similar impact was discernable in RUN4 (Fig. 10C), but cutoff in RUN5 resulted in a complex trend, increased first and then decreased (Fig. 10C). For the downstream segment, the temporal trend of M_c after cutoff varied differently. In RUN3, it decreased shortly and then increased continuously till the end of the experiment (Fig. 10B). In RUN4, it simply increased (Fig. 10C). In RUN5, it increased first with less degree and then decreased (Fig. 10D).

Visually comparing RUN2 with runs 3–5, lateral migration over the entire experimental periods in runs 3–5 was ostensibly more intensive than that in RUN2 in the upstream and downstream segments (Fig. 11). The abandoned channel segment in runs 3–5 generally remained unchanged with some local migration. The new cutoff channel evolved for 35, 27, and 22 h in runs 3, 4, and 5 respectively. They already showed some degree of lateral migration, indicating their relatively quick adjustment after creation.

3.3.2. Scour areas

Erosion in all experiments was dominated by bank erosion and collapse, leading to the continuous retreat of bank lines with time (Fig. 12). In RUN2 without neck cutoff, scour was the most intensive in the upstream segment and increased linearly with time (Figs. 12A and 13A). The magnitude of erosion in the bend segment was originally lower than that of the downstream one but quickly overpassed that of the latter and then increased gradually. Temporal patterns of erosion volumes in the three runs with neck cutoff were different. In RUN3,

the bend segment experienced the most intensive erosion before and after cutoff, though the erosion rate decreased significantly after cutoff (Figs. 12B and 13B). The trend of erosion in the upstream segment did not change, while the erosion volume in the downstream one was augmented after cutoff. Over the entire experimental period, the erosion volume in the upstream segment was about 5 times higher than that in the downstream one.

In runs 4 and 5, the erosion volume in the upstream and bend segments was close and obviously higher than that in the downstream one (Fig. 13C and D). Before cutoff, temporal changes of the erosion volume in the two runs were similar, though the rate of the change was higher in RUN5 than that in RUN4 (Fig. 12C and D). The neck cutoff reduced the magnitude of erosion in both segments with a higher reduction rate of change shown in the bend segment, indicating the reduced channel dynamics in the bend segment because of cutoff. Interestingly, in the downstream segment, cutoff indeed enhanced erosion by triggering a significant left bank erosion in both runs soon after neck cutoff (Figs. 12C and D, 13C and D).

3.3.3. Cross sections of the channels

In RUN2 without neck cutoff, the width/depth ratio remained almost unchanged over time in all three segments and was slightly higher in the downstream segment than in the other two (Fig. 14A). However, neck cutoff had a very significant impact on cross section morphology in runs 3–5. In RUN3, occurrence of cutoff increased the ratio of three representative cross sections in the order of upstream, bend, and
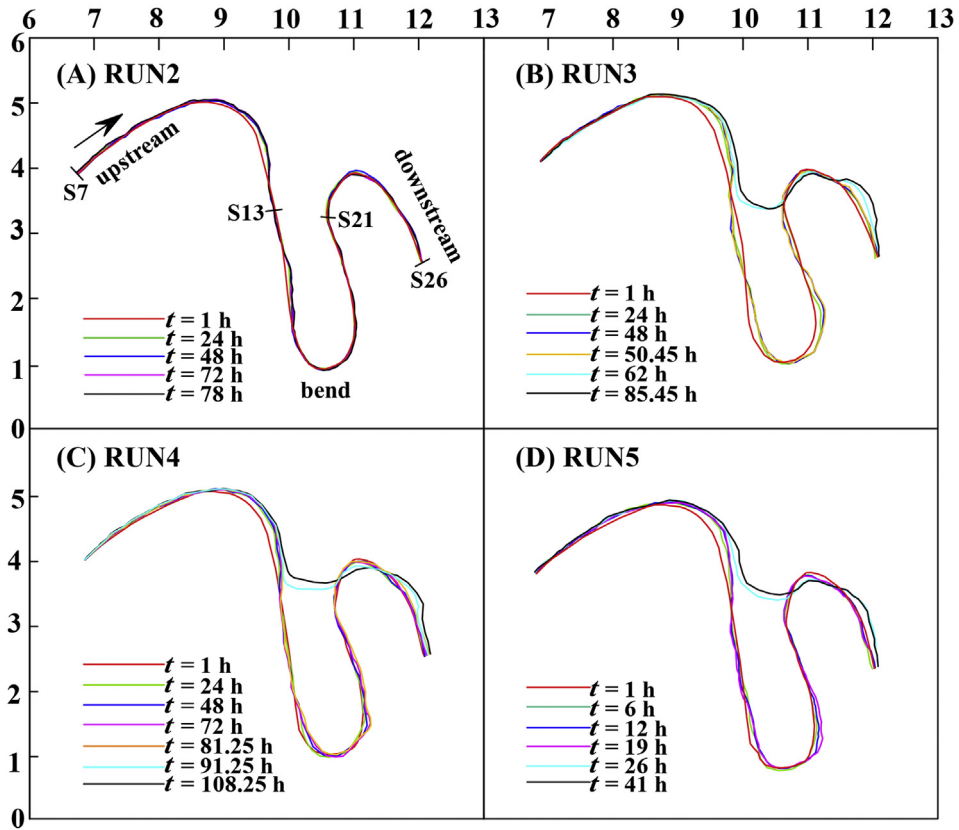
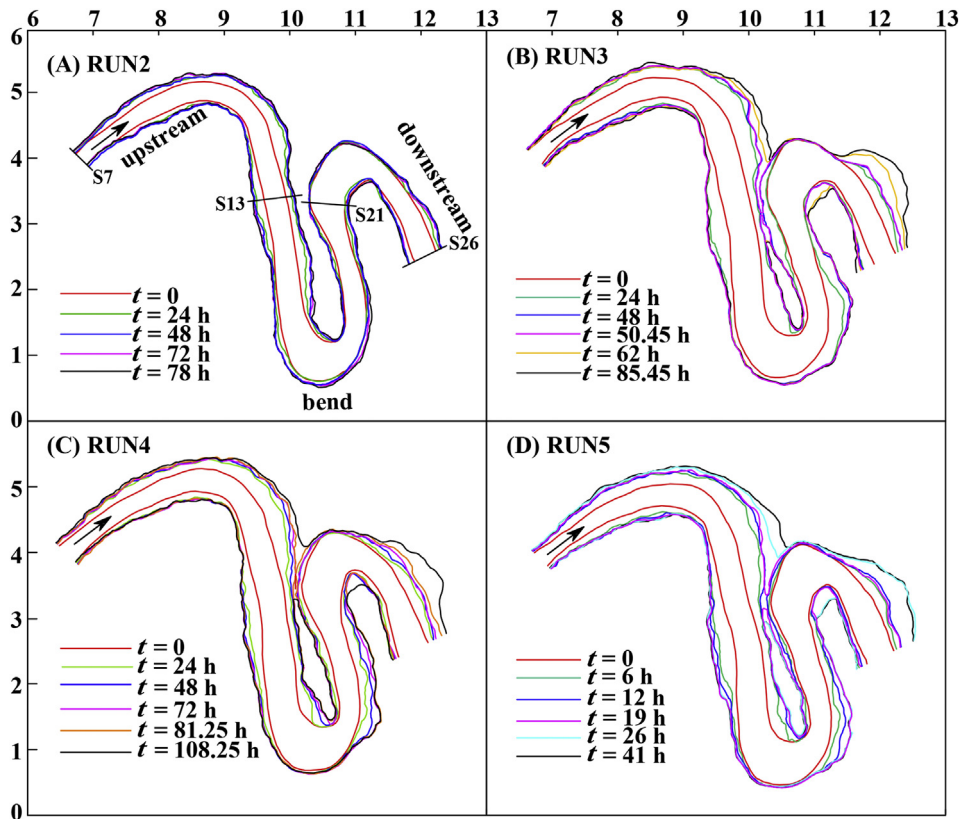**Fig. 11.** Temporal changes of the meandering channel centerline over time in runs 2–5.

Fig. 12. Temporal changes of bank lines during experiments (unit of horizontal and vertical coordinate: meter) in runs 2–5.
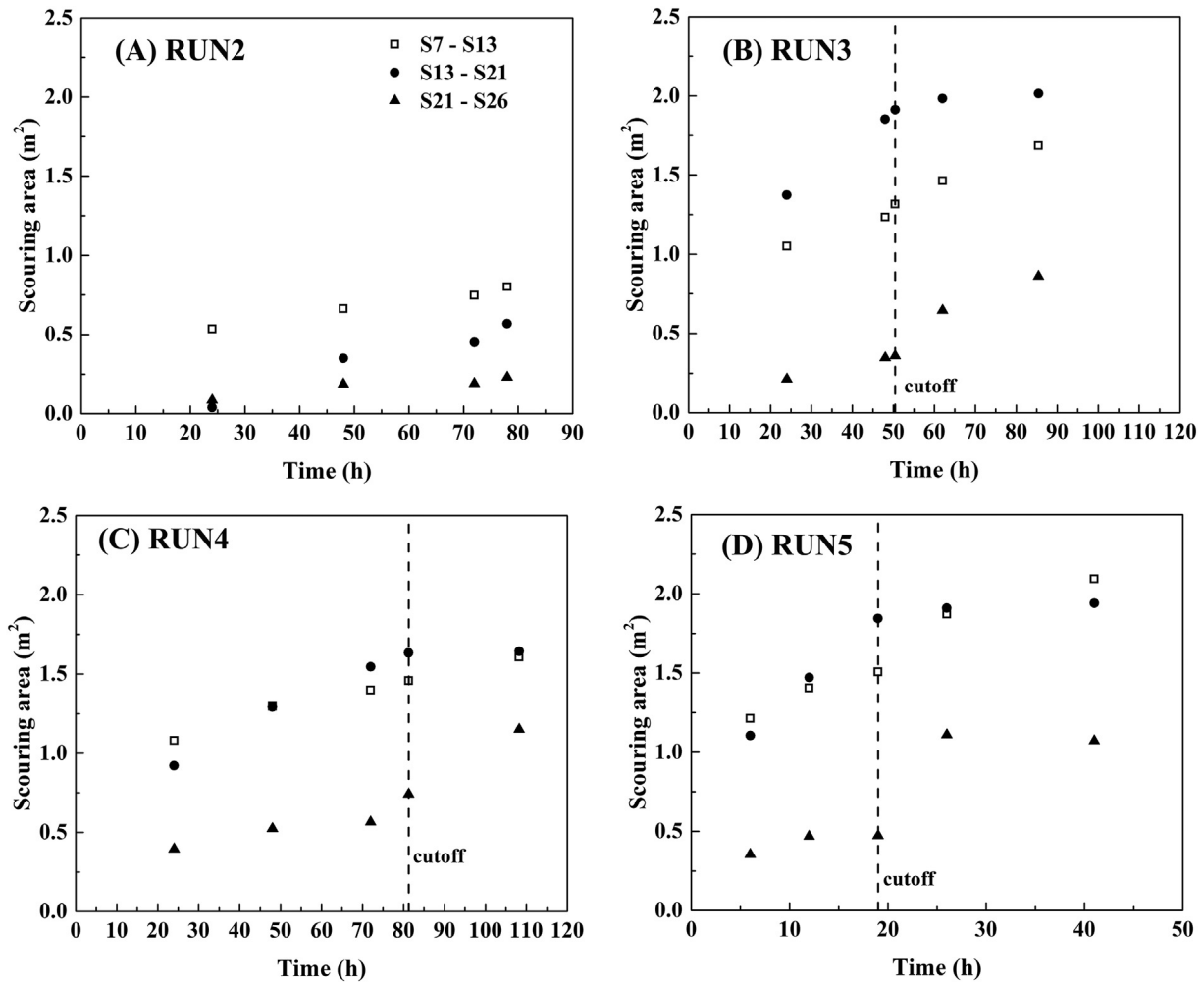
Fig. 13. Temporal changes of scouring area at S7–S13 (upstream segment), S13–S21 (bend segment), and S21–S26 (downstream segment) in runs 2–5.

downstream segments (Fig. 14B). The ratio was increased by 5.7 times in the upstream segment, whereas by about 3.6 times in the other two. After neck cutoff, the width/depth ratio in upstream and downstream segments still increased with a much lesser rate of about 1.1 and 1.3 for runs 4 and 5 respectively. This ratio in the bend segment was slightly decreased, signifying the reduced activity in it.

In RUN4, the increase of the width/depth ratio during and after cutoff was lesser than that in RUN3 (Fig. 14B and C), but the highest rate of increase still fell on the cross section in the upstream segment. After neck cutoff, this ratio increased in the upstream and downstream segments by 1.06 and 1.73 times respectively, showing a higher degree of morphologic response of the downstream channel segment. Similar to that in RUN3, the ratio in the abandoned segment slightly decreased in RUN4. This ratio in RUN5 demonstrated similar patterns of changes during and after neck cutoff to those in RUN3, except that the highest ratio during cutoff was that in the bend segment (Fig. 14D).

4. Discussions

4.1. Limitations of our flume experiments

Although we successfully captured the processes of neck cutoff in three experimental runs and the subsequent channel adjustment in relatively short time periods, our experiments suffered some limitations. First, bank materials in our laboratory flume were noncohesive and relatively uniform medium sands ($d_{50} = 0.327$ mm). They are different from natural meandering rivers (e.g., the Qigongling Bend)

where bank material composition is nonuniform, containing clay and silt in the upper layer with vegetation roots and coarse sand in the lower layer. The latter may significantly affect formation and evolution of meandering rivers (Moor et al., 2010; Tal and Paola, 2010; Güneralp et al., 2012), as well as cutoff processes (Hooke, 2004; Braudrick et al., 2009; van Dijk et al., 2012; Han and Endreny, 2014; Eekhout and Hoitink, 2015). Second, no sediment supply was involved in our experiments. Third, only constant discharges were used in our experiments, while in natural meanders, they are variable. Finally, we did not consider the Froude similarity criteria of the flow. As such, we cannot determine the scaling time between flume experiment and Qigongling Bend in nature.

Nonetheless, we argue that simplified hydrological, sediment, and boundary conditions in our flume experiments should not shade their scientific values. As our experiments were all performed over a mobile bed, the clear input flow was able to entrain sediment from the bed of the upstream section about 10 m long and entered the study reach at S7 (Fig. 2A) as a sediment-laden flow. It could also reproduce ripples and dunes on the bed, giving rise to a variety of local deposition within the study reach. Thus, the flow in our experiments is similar to that in meanders below dams in many places of the world. Earlier flume experiments (Braudrick et al., 2009) have shown that a flow of variable discharges is not necessarily required to sustain channel meandering and generate chute cutoff in flume experiments. Given that our experiments aimed at understanding the process of neck cutoff and the subsequent channel adjustment, constant discharges used in our experiments were sufficient and the time duration of each experiment does not
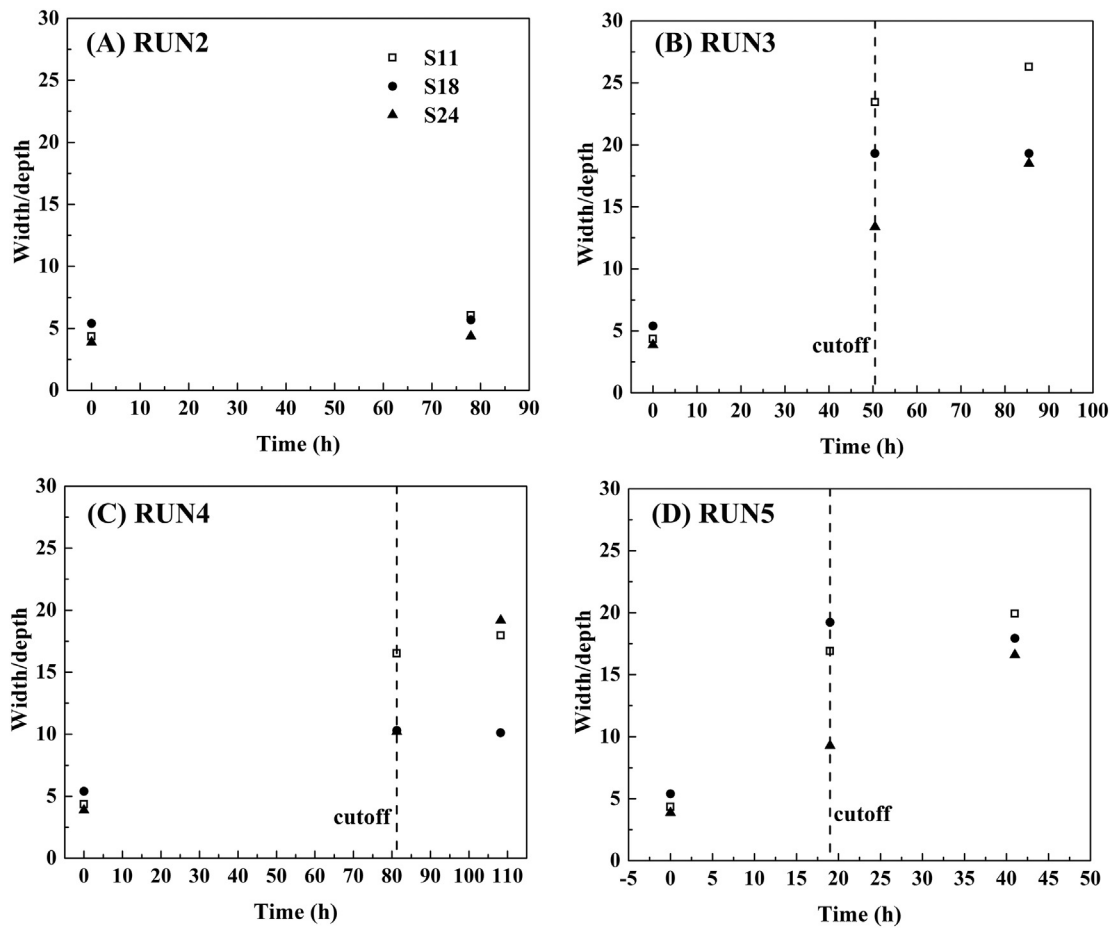
Fig. 14. Temporal change of width-depth ratios in three representative cross sections in runs 2–5.

have to match a real time duration. Thus far, neck cutoff has only been examined based on field observation and model simulation (Hooke, 1995; Sun et al., 1996; Gay et al., 1998; Fares, 2000; Camporeale et al., 2008; Micheli and Larsen, 2011; Schwenk et al., 2015; Konsoer and Richards, 2016), and there is no laboratory flume experiments on the neck cutoff process in has been performed. Without attempting to predict the real hydraulic conditions controlling neck cutoff, based on uniform bed and bank materials, we successfully reproduced the occurrence of neck cutoff in highly sinuous meanders excavated only based on geometric similarity in a laboratory flume. This success allowed us to reveal some key characteristics controlling the process of neck cutoff and the associated channel adjustment as described below.

4.2. Implications of our flume experiments

4.2.1. A hydraulic control factor

Generally, discharges in flume experimental runs triggering neck cutoff were 50% to 600% higher than those in runs without neck cutoff (Table 1), suggesting that higher discharges are needed for neck cutoff. This seems consistent with earlier findings that a large increase of discharge during flood seasons is the main cause to trigger neck and

chute cutoff (Hooke, 1995; Gay et al., 1998; Hooke, 2004; Micheli and Larsen, 2011; Li et al., 2017). Among three runs with neck cutoff, RUN3 had the lowest discharge, while RUN5 had the highest. The time duration they took to initiate neck cutoff was 50.45, 81.25, and 19 h respectively (Fig. 5). This mismatch between discharges and time durations suggests that other factors might also control the process of neck cutoff. Reviewing the initial conditions of these three runs showed that channel slope might be one. Using the local surface slopes before neck cutoff, which were 0.00270, 0.00219, 0.00180 for runs 3, 4, and 5 respectively, we calculated their local unit stream power P and found that P was around 0.053 N·s^{-1} in all three runs (Table 3). These similar local P values clearly suggested that local unit stream power is essentially a control factor for the occurrence of neck cutoff. This confirmed the earlier field observation that cutoff tends to occur in the location where the unit stream power is the largest (Lewis and Lewin, 1983; Hooke, 1995); and we should add an additional hydraulic factor that controls the initiation of neck cutoff to the existing list of control factors for cutoff, such as river planform geometry, river bank heterogeneity, and vegetation (Gay et al., 1998; Camporeale et al., 2008; Constantine et al., 2009; Micheli and Larsen, 2011; Zinger et al., 2011; van Dijk et al., 2012; Thompson, 2003; Li and Gao, 2019).

Table 3
Critical hydraulic condition of neck cutoff in runs 3–5.

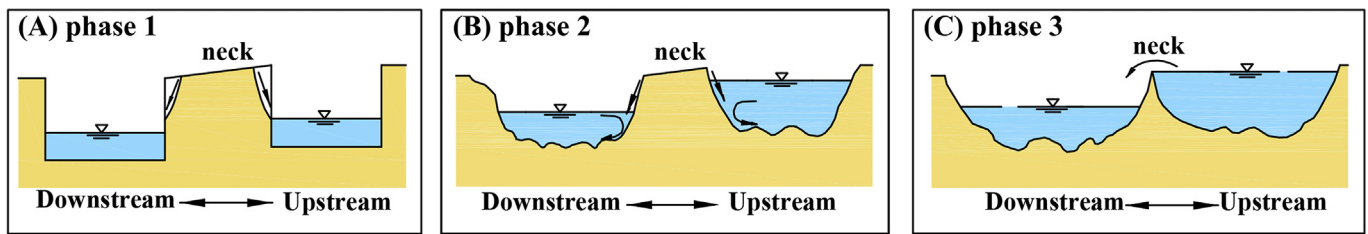| Run	S_r (‰)	Duration (h)	Q (m³/s)	Water head between upstream and downstream (cm)	Hydraulic gradient S	Unit stream power P (N·s^{-1})
3	1.0	50.45	0.0020	2.07	0.00270	0.0530
4	0.8	81.25	0.0025	1.68	0.00219	0.0537
5	1.7	19.00	0.0030	1.38	0.00180	0.0530

Fig. 15. A conceptual model of the neck cutoff process: (A) phase 1, (B) phase 2, and (C) phase 3.

4.2.2. Insight into mechanisms of neck cutoff

Although discharges in runs 3, 4, and 5 with neck cutoff were relatively high, their associated water depths were merely 41%, 46%, and 54% of the bankful depth respectively (Table 1), suggesting that discharges with moderate magnitudes are sufficient to induce neck cutoff given that the experimental duration is long enough. This is at odds with previous observations that overbank flow formed by low-frequency discharges is the main reason for the occurrence of neck cutoff (Erskine et al., 1992; Hooke, 1995, 2004; Gay et al., 1998; Li et al., 2017). It also implies that bank erosion on both sides of the neck caused by moderate discharges, which was evidenced by ubiquitous bankline retreat in runs 3–5 (Fig. 12), is a key mechanism leading to neck cutoff. Therefore, discharges that are capable of generating neck cutoff may not necessarily be the bankful discharge.

The fact that temporal trends of neck cutoff process in the three runs were similar (Fig. 5) allowed us to develop a conceptual model characterizing the mechanics of neck cutoff process that involves three phases (Fig. 15). In phase 1, which is within 10% to 26% of the total duration of neck cutoff development, upstream and downstream banks of the neck are eroded fast mainly through bank collapse, causing intensive widening of the cross sections on both sides (Fig. 6) and quick neck width reduction (Fig. 5). The collapsed bank materials could not be completely evacuated by the moderate discharges. Consequently, some accumulated on the bank toe, which serves as a temporary protection on banks. In phase 2, the protection reduced the intensity of bank erosion. As a result, the rates of cross section widening and neck width reduction decrease (Figs. 5 and 6), leading to a much longer duration ranging from about 70% to 90% of the total duration. In phase 3, significantly reduced neck width increases head gradient on the thinned neck (Fig. 6), giving rise to the water head differences of 2.07, 1.68, and 1.38 cm for runs 3, 4, and 5, respectively. This gradient is caused by water level difference between upstream and downstream of the neck, which is equivalent to the product of the centerline length and the channel slope. It generates seepage flow erosion through non-cohesive sand at the neck (Han and Endreny, 2014), causing neck cutoff by connecting upstream and downstream sides of the neck in a very short time period. In runs 3, 4, and 5, this time period was 0.8%, 0.3%, and 2.6% of the total experimental time respectively. This explains why, in natural meandering rivers, neck cutoff is extremely difficult to be observed.

4.2.3. Interaction between neck cutoff and its neighboring channels

In all three runs with neck cutoff, we observed two general patterns. First, the cutoff channel expanded quickly immediately after neck cutoff (Fig. 7A and B). This expansion took <1% of the time duration for the channel becoming stable (Fig. 8A and B). After this stage, both rate and magnitude of channel width broadening decreased quickly, taking about 10% of the total time. The width of the cutoff channel continuously widened, which was followed by a relatively long period for the channel gradually reaching a stable stage (Figs. 7C and 8). This fast channel adjustment after neck cutoff is consistent with previous field observation (Hooke, 1995; Li and Gao, 2019) and is a key characteristic of the cutoff channel adjustment. Second, our experiments with cutoff also showed that neck cutoff enhanced upstream and downstream channel erosion, causing channel width widening and increased

width/depth ratio (Figs. 13 and 14). Regarding the upstream section, our results are consistent with field observations in two meandering rivers in northwest England (Hooke, 1995), but opposite those in the White River in Arkansas, USA (Konsoer and Richards, 2016). We think this complexity could be caused by different rates of sediment supply, which needs to be investigated further. The downstream adjustment has not been reported in meanders with neck cutoff, though for chute cutoff, sediment deposition was widely documented (e.g., Eekhout and Hoitink, 2015; Zinger et al., 2011). This seems to imply that neck cutoff affects its downstream channel in a different way from chute cutoff. At least one possible explanation is that when chute cutoff happens, a large amount of bank materials may be eroded and carried in a short time period to the downstream channel, such that flow cannot carry all of them, resulting in deposition, while the process of neck cutoff gradually erodes bank materials, which allows flow to carry them during a relatively long period and leaves little bank material for flow to entrain when neck cutoff happens.

4.3. Implication for the Qigongling Bend

Although our experiments showed some general scientific values regarding the process of neck cutoff and the subsequent adjustment of the cutoff channel, they may also provide some meaningful information for the specific bend that was used to create our flume meanders. Probably the most important implication from our experiments is that the key process that can shape the Qigongling Bend is bank erosion. Thus, for the local management agencies, the most efficient measure of avoiding neck cutoff of this bend might be bank protection. Currently, a section of this big bend that has not been protected and bank erosion (mainly bank collapse) has been very active. According to Fig. 5, this erosion process could continue with a high rate. Although plants on top of the bank may decelerate this rate to some degree, the bank erosion is mainly caused by fluvial erosion on bank toe, which will cause collapse of the upper layer (Xia et al., 2014, 2016). Therefore, implementing bank protection structure is apparently imperative.

5. Conclusions

In this study, we conducted laboratory experiments to investigate the process of neck cutoff and the associated channel adjustment. By artificially creating a highly sinuous meander channel based on the Qigongling Bend in the lower Jingjiang River, China, using a geometric similarity method, we successfully achieved neck cutoff in three out of five flume experiments. Although constant discharges without sediment input were used in these experiments, the findings from these experiments are valuable for understanding the process and mechanics of neck cutoff and the associated channel adjustment, which are summarized as follows:

• Neck cutoff is essentially controlled by bank erosion caused by moderate flows in meandering channels. Bank erosion is active on both sides of the neck. The reduction rate of neck width depends on whether or not sediment accumulates at the bank toe. Without it, bank erosion may be controlled by bank collapse, leading to a fast narrowing rate of

the neck. The subsequent sediment accumulation may reduce this rate, but still maintain the neck narrowing process. The true neck cutoff happens in a very short time period and is caused by increased head gradient owing to water level difference on both sides of the neck and on the thinning of the neck. This mechanism explains the difficulty of observing neck cutoff in natural meandering rivers.

- The cutoff channel increases in size promptly after neck cutoff because of increased local slope, which keeps a relatively high local unit stream power in the cutoff channel. The subsequent channel development is continuously fast with a decreased rate. Then, the cutoff channel gradually reaches a stable stage in which its morphology approximately remains unchanged. This finding confirms the previous field observation in natural meanders.
- Neck cutoff enhanced bank erosion and channel widening in upstream and downstream channels. The upstream impact supports some earlier field observation but is at odds with others. We believe this is mainly caused by different sediment supply rates in different rivers and needs to be further examined. The downstream impact likely reflects the fact that sediment-laden flow in our experiments is below capacity, such that it is still capable of scouring the downstream channel.

These findings provide insight into understanding the process of neck cutoff and set up a valuable benchmark for future flume studies on neck cutoff. Practically, our experiments provide scientific evidence of possibly supporting future management practice of implementing bank protection structure to the banks of the Qigongling Bend in the lower Jingjiang River.

Acknowledgements

References

Abernethy, B., Rutherfurd, I.D., 2000. The effect of riparian tree roots on the mass-stability of riverbanks. Earth Surf. Process. Landf. 25, 921–937.

Allen, J.R.L., 1965. A review of the origin and characteristics of recent alluvial sediments. Sedimentology 5, 89–191.

Billi, P., Demissie, B., Nyssen, J., Moges, G., Fazzini, M., 2018. Meander hydromorphology of ephemeral streams: similarities and differences with perennial rivers. Geomorphology 319, 35–46.

Braudrick, C.A., Dietrich, W.E., Leverich, G.T., Sklar, L.S., 2009. Experimental evidence for the conditions necessary to sustain meandering in coarse-bedded rivers. Proc. Natl. Acad. Sci. 106, 16936–16941.

Camporeale, C., Perucca, E., Ridolfi, L., 2008. Significance of cutoff in meandering river dynamics. J. Geophys. Res. 113, F01001. https://doi.org/10.1029/2006JF000694.

Church, M., 2002. Geomorphic thresholds in riverine landscapes. Freshw. Biol. 47, 541–557.

Constantine, J.A., McLean, S.R., Dunne, T., 2009. A mechanism of chute cutoff along large meandering rivers with uniform floodplain topography. Geol. Soc. Am. Bull. 122, 855–869.

Constantine, J.A., Dunne, T., Ahmed, J., Legleiter, C., Lazarus, E.D., 2014. Sediment supply as a driver of river meandering and floodplain evolution in the Amazon Basin. Nat. Geosci. 7, 899–903.

van Dijk, W.M., van de Lageweg, W.I., Kleinhans, M.G., 2012. Experimental meandering river with chute cutoffs. J.Geophys. Res. Earth Surf. 117, F03023. https://doi.org/10.1029/2011JF002314.

van Dijk, W.M., Schuurman, F., van de Lageweg, W.I., Kleinhans, M.G., 2014. Bifurcation instability and chute cutoff development in meandering gravel-bed rivers. Geomorphology 213, 277–291.

Dulal, K.P., Shimizu, Y., 2010. Experimental simulation of meandering in clay mixed sediments. J. Hydro-environ. Res. 4, 329–343.

Eekhout, J.P.C., Hoitink, A.J.F., 2015. Chute cutoff as a morphological response to stream reconstruction: the possible role of backwater. Water Resour. Res. 51, 3339–3352.

Erskine, W.D., Mcfadden, C., Bishop, P., 1992. Alluvial cutoffs as indicators of former channel conditions. Earth Surf. Process. Landf. 17, 23–37.

Fares, Y.R., 2000. Changes of bed topography in meandering rivers at a neck cutoff intersection. J. Environ. Hydrol. 8, 1–18.

Friedkin, J.F., 1945. Laboratory Study of the Meandering of Alluvial Rivers. U.S. Waterways Experiment Station, Vicksburg, Mississippi.

Gay, G.R., Gay, H.H., Gay, W.H., Martinson, H.A., Meade, R.H., Moody, J.A., 1998. Evolution of cutoffs across meander necks in Powder River, Montana, USA. Earth Surf. Process. Landf. 23, 651–662.

Grenfell, M.C., Nicholas, A.P., Aalto, R., 2014. Mediative adjustment of river dynamics: the role of chute channels in tropical sand-bed meandering rivers. Sediment. Geol. 301, 93–106.

Güneralp, İ., Abad, J.D., Zolezzi, G., Hooke, J., 2012. Advances and challenges in meandering channels research. Geomorphology 163–164 (1–9).

Han, B., Endreny, T.A., 2014. Detailed river stage mapping and head gradient analysis during meander cutoff in a laboratory river. Water Resour. Res. 50, 1689–1703.

Hooke, J.M., 1995. River channel adjustment to meander cutoffs on the River Bollin and River Dane, northwest England. Geomorphology 14, 235–253.

Hooke, J.M., 2004. Cutoffs galore!: occurrence and causes of multiple cutoffs on a meandering river. Geomorphology 61, 225–238.

Hooke, J.M., 2007. Complexity, self-organisation and variation in behaviour in meandering rivers. Geomorphology 91, 236–258.

Hooke, J.M., 2013. River Meandering. Academic Press, San Diego, CA.

Howard, A.D., 2009. How to make a meandering river. Proc. Natl. Acad. Sci. 106, 17245–17246.

Jia, D., Shao, X., Wang, H., Zhou, G., 2010. Three-dimensional modeling of bank erosion and morphological changes in the Shishou bend of the middle Yangtze River. Adv. Water Resour. 33, 348–360.

Konsoer, K.M., Richards, G., 2016. Planform evolution of neck cutoffs on elongate meander loops, White River, Arkansas, USA. In: Constantinescu, G., Garcia, M., Hanes, D. (Eds.), River Flow 2016. Taylor & Francis Group, Boca Raton, St. Louis, USA.

Krzeminska, D., Kerkhof, T., Skaalsveen, K., Stolte, J., 2019. Effect of riparian vegetation on stream bank stability in small agricultural catchments. Catena 172, 87–96.

Lewis, G.W., Lewin, J., 1983. Alluvial cutoffs in Wales and the Borderlands. In: Collinson, J.D., Lewin, J. (Eds.), Modern and Ancient Fluvial Systems, pp. 145–154.

Li, Z., Gao, P., 2019. Channel adjustment after artificial neck cutoffs in a meandering river of the Zoige basin within the Qinghai-Tibet Plateau, China. Catena 172, 255–260.

Li, Z., Yu, G.A., Brierley, G., Wang, Z., Jia, Y., 2017. Migration and cutoff of meanders in the hyperarid environment of the middle Tarim River, northwestern China. Geomorphology 276, 116–124.

Micheli, E.R., Larsen, E.W., 2011. River channel cutoff dynamics, Sacramento River, California, USA. River Res. Appl. 27, 328–344.

Micheli, E.R., Kirchner, J., Larsen, E., 2004. Quantifying the effect of riparian forest versus agricultural vegetation on river meander migration rates, Central Sacramento River, California, USA. River Res. Appl. 20, 537–548.

Millar, R.G., 2000. Influence of bank vegetation on alluvial channel patterns. Water Resour. Res. 36, 1109–1118.

Moor, J.J.W.D., Balen, R.T.V., Kasse, C., 2010. Simulating meander evolution of the Geul River (the Netherlands) using a topographic steering model. Earth Surf. Process. Landf. 32, 1077–1093.

Pan, C.S., Shi, S.C., Duan, W.Z., 1978. A study of the channel development after the completion of artificial cutoffs in the middle Yangtze River. Sci. Sinica 21, 783–804.

Parker, G., Shimizu, Y., Wilkerson, G.V., Eke, E.C., Abad, J.D., Lauer, J.W., Paola, C., Dietrich, W.E., Voller, V.R., 2011. A new framework for modeling the migration of meandering rivers. Earth Surf. Process. Landf. 36, 70–86.

Peakall, J., Ashworth, P.J., Best, J.L., 2007. Meander-bend evolution, alluvial architecture, and the role of cohesion in sinuous river channels: a flume study. J. Sediment. Res. 77, 197–212.

Perucca, E., Camporeale, C., Ridolfi, L., 2007. Significance of the riparian vegetation dynamics on meandering river morphodynamics. Water Resour. Res. 43, W03430. https://doi.org/10.1029/2006WR005234.

Schumm, S., 1985. Patterns of alluvial rivers. Annu. Rev. Earth Planet. Sci. 13, 5–27.

Schumm, S.A., Khan, H.R., 1972. Experimental study of channel patterns. Geol. Soc. Am. Bull. 83, 1755–1770.

Schwenk, J., Lanzoni, S., Foufoula-Georgiou, E., 2015. The life of a meander bend: connecting shape and dynamics via analysis of a numerical model. J. Geophys. Res. Earth Surf. 120, 690–710.

Seminara, G., 2006. Meanders. J. Fluid Mech. 554, 271–297.

Simon, A., Collison, A.J.C., 2002. Quantifying the mechanical and hydrologic effects of riparian vegetation on streambank stability. Earth Surf. Process. Landf. 27, 527–546.

Słowik, M., 2016. The influence of meander bend evolution on the formation of multiple cutoffs: findings inferred from floodplain architecture and bend geometry. Earth Surf. Process. Landf. 41, 626–641.

Smith, C.E., 1998. Modeling high sinuosity meanders in a small flume. Geomorphology 25, 19–30.

Smith, L.M., Winkley, B.R., 1996. The response of the Lower Mississippi River to river engineering. Eng. Geol. 45, 433–455.

Song, X., Xu, G., Bai, Y., Xu, D., 2016. Experiments on the short-term development of sine-generated meandering rivers. J.Hydro-environment Res. 11, 42–58.

Stolum, H.H., 1996. River meandering as a self-organisation process. Science 271, 1710–1713.

Stolum, H.H., 1998. Planform geometry and dynamics of meandering rivers. Geol. Soc. Am. Bull. 110, 1485–1498.

Sun, T., Meakin, P., Jossang, T., 1996. A simulation model for meandering rivers. Water Resour. Res. 32, 2937–2954.

Tal, M., Paola, C., 2010. Effects of vegetation on channel morphodynamics: results and insights from laboratory experiments. Earth Surf. Process. Landf. 35, 1014–1028.

Thompson, D.M., 2003. A geomorphic explanation for a meander cutoff following channel relocation of a coarse-bedded river. Environ. Manag. 31, 385–400.

Tiffany, J.B., Nelson, G.A., 1939. Studies of meandering of model-streams. Trans. Am. Geophys. Union 20, 644–649.

Viero, D.P., Dubon, S.L., Lanzoni, S., 2018. Chute Cutoffs in Meandering Rivers: Formative Mechanisms and Hydrodnamic Forcing. International Association of Sedimentologists (IAS Special Publications).

Visconti, F., Camporeale, C., Ridolfi, L., 2010. Role of discharge variability on pseudomeandering channel morphodynamics: results from laboratory experiments. J. Geophys. Res. 115, F04042. https://doi.org/10.1029/2010JF001742.

Wang, Z., Li, Z., Xu, M., Yu, G., 2016. River Morphodynamics and Stream Ecology of the Qinghai-Tibet Plateau. CRC Press, Taylor & Francis Ltd.

Xia, J., Zong, Q., Deng, S., Xu, Q., Lu, J., 2014. Seasonal variations in composite riverbank stability in the lower Jingjiang Reach, China. J. Hydrol. 519, 3664–3673.

Xia, J., Deng, S., Lu, J., Xu, Q., Zong, Q., Tan, G., 2016. Dynamic channel adjustments in the Jingjiang Reach of the Middle Yangtze River. Sci. Rep. 6, 22802.

Xia, J., Deng, S., Zhou, M., Lu, J., Xu, Q., 2017. Geomorphic response of the Jingjiang Reach to the three Gorges Project operation. Earth Surf. Process. Landf. 42, 866–876.

Xu, D., Bai, Y., 2013. Experimental study on the bed topography evolution in alluvial meandering rivers with various sinuousnesses. J. Hydro-environ. Res. 7, 92–102.

Yang, C., Cai, X., Wang, X., Yan, R., Zhang, T., Zhang, Q., Lu, X., 2015. Remotely sensed trajectory analysis of channel migration in lower Jingjiang reach during the period of 1983–2013. Remote Sens. 7, 16241–16256.

Yin, X., 1965. Preliminary experiment study on formation and evolution of meandering river. Acta Geogr. Sin. 31, 287–303.

Zhou, F., 1994. Historical evolution of Yunmeng marsh and Jingjiang delta. J. Lake Sci. 6, 22–32 (in Chinese).

Zhu, H., Hu, X., Li, Z., Song, L., Li, K., Li, X., Li, G., 2018. The influences of riparian vegetation on bank failures of a small meadow-type meandering river. Water 10, 692.

Zinger, J.A., Rhoads, B.L., Best, J.L., 2011. Extreme sediment pulses generated by bend cutoffs along a large meandering river. Nat. Geosci. 4, 675–678.